Novel Fault Diagnostic Technique for Permanent Magnet Synchronous Machines Using Electromagnetic Signature Analysis

Yao Da, *Student Member*, *IEEE* and Mahesh Krishnamurthy, *Member*, *IEEE*

Electric Drives and Energy Conversion Laboratory, Electrical and Computer Engineering Department,
Illinois Institute of Technology, 3301 S. Dearborn St., Chicago, IL 60616
E-mail: kmahesh@ece.iit.edu, URL: www.drives.ece.iit.edu/

***Abstract*—This paper proposes a novel alternative scheme for permanent magnet synchronous machine (PMSM) health monitoring and multi-faults detection using direct flux measurement with search coils. Phase current spectrum is not used for analysis and therefore it is not influenced by power supply introduced harmonics any more. In addition, it is also not necessary to specify load condition for accurate diagnosis. In this study, numerical models of a healthy machine and of machines with various faults are developed and examined. Simulation by means of a two-dimensional finite-element analysis (FEA) software package is presented to verify the application of the proposed method over different motor operation conditions.**

***Keywords*—Permanent Magnet Synchronous Machine, Search Coils, Fault Diagnosis, Finite Element Analysis.**

I. INTRODUCTION

Over the past decade, Permanent Magnet Synchronous Machines (PMSMs) have become a preferred choice in the industry, especially where high performance is required. This is because they have higher efficiency, high output power to volume ratio, high torque to current ratio, etc. While the PMSM is relatively robust, some failures are inevitable. Several faults can be seen in PMSMs including eccentricity, bearing failure, demagnetization of permanent magnets, short circuit in the stator or armature winding etc. This necessitates health monitoring and fault diagnosis of the machine to maintain their performance and increase their lifetime.

Since traditional off-line machine fault detection and diagnostic methods don't allow for frequent testing and are financially impractical, many on-line methods have been proposed. Mainstream methods are based on spectrum analysis: armature current spectrum [1]-[3] or vibration spectrum [4]-[5]. The main advantage of this kind of method is that they are noninvasive, no additional hardware required and do not need an accurate machine model. However, inverters may add unpredictable harmonics to the current spectrum. And in some applications when the machine speed is not stationary, it is hard to determine the harmonic orders. Penman et al [6]-[7] developed an approach using a search coil to measure axial leakage flux signal of induction machine to detect some common faults in induction machines, such as broken rotor bars, wound rotor short circuit, inter-turn short circuit, eccentric operation, etc. However this paper also acknowledges that the technique is not suitable for inverter fed systems due to the additional harmonic content from the power supply. Another kind of method uses negative/zero current [8]-[9], negative/zero impedance [10], or negative/zero voltage [11] as indicators. These indicators are sensitive to machine asymmetry so that faults caused unbalance signals can be detected. However, any asymmetry caused by the machine structure or the power supply's unbalance could influence the fault detection. Parameter estimation [12]-[13] is another scheme that is able to perform online fault diagnosis through detecting abnormal physical parameters. The disadvantage of this scheme is that an accurate machine model is required.

In this paper, an alternative multi-faults detection method using search coils is proposed. These invasive coils are wound around armature teeth, so they typically need to be installed during manufacturing. But its immunity to high frequency harmonics makes it suitable for inverter/rectifier fed motors or generators, such as wind turbines and automotive systems. In addition, this method does not require the knowledge of machine parameters. Since the air gap flux is directly measured in this method, it provides much more diagnosis reliability. In order to verify the validity of the presented scheme, several scenarios have been studied for a PMSM. Models with eccentricity, armature winding short-turn, demagnetization running with different torque have been modeled by Finite Element Analysis (EFA) where geometrical and physical characteristics of different parts of the machine are considered.

II. MODEL DEVELOPMENT FOR PROPOSED TECHNIQUE

Figure 1 shows the cross section of the machine utilized in this paper. This three phase Y-connected machine has a concentrated armature winding and a sinusoidal back EMF. Details of its specifications of the presented PMSM have been summarized in Table II in appendix of this paper.

Twelve search coils are wound around each tooth of this machine. Their voltages are recorded and the amplitude and phase of their first harmonic are taken for further analysis. Number of required search coils for different fault case is

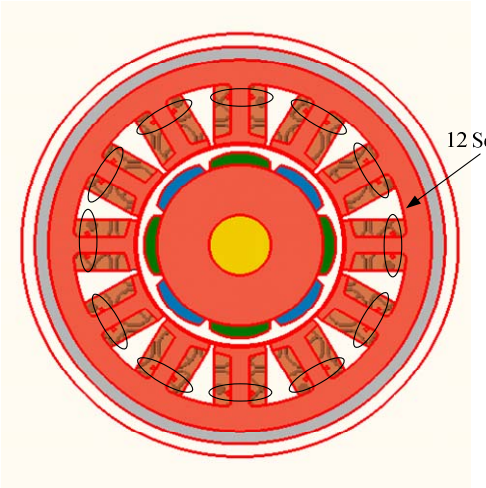

Fig 1. Geometric configuration of the PMSM

TABLE I

NUMBER OF REQUIRED SEARCH COILS FOR FAULTS

Fault case	Number of search coils required
Eccentricity	3
Demagnetization	Number of poles
Phase failure	Number of phases
Inter-turn fault	Number of solenoids

given in Table I. To analyze all the given four kinds of fault cases, maximum number of search coils, 12, is chosen.

III. ARMATURE REACTION DECOUPLING

What each search coil measures is a vector summation of flux due to permanent magnets and armature coils induced flux, when there is no saturation. To analyze the reason of flux unbalance, it is required to couple these two parts. The phasor diagram for the operation of the PMSM as a generator is shown in Fig 2. When no load is mounted and the rotor is revolving at the synchronous speed, back EMF E_r at the search coil is produced by the field MMF F_r in each phase. The MMF distribution can be described as space vectors, where the EMFs are time phasors. The superposition of the filed MMF and the armature MMF, known as armature reaction, produces resultant air-gap MMF F_{rs}, which is the vector sum of F_r and F_s. Additionally, this MMF is responsible for the resultant air-gap flux which induces a back EMF in the search coil under load, denominated as E_{rs} in Fig 2.

The machine used in this study is controlled using vector control scheme [14] where phase current I has the same direction of q axis. Thus the armature reaction voltage E_s leads E_r by 90 degree. So they can be decoupled as following:

$$E_r = E_{rs}\cos\theta \tag{1}$$

and

$$E_s = E_{rs}\sin\theta \tag{2}$$

where θ is angle between the rotor MMF and the resultant air-gap MMF.

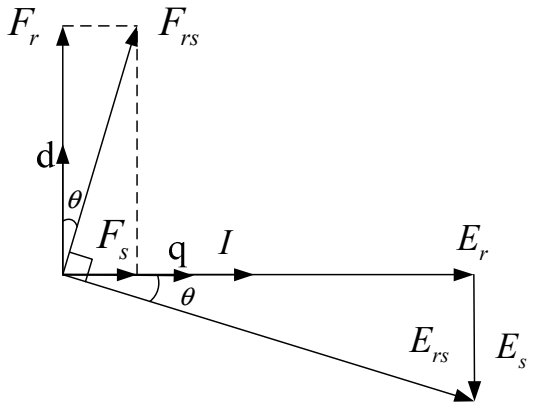

Fig 2. Phasor/vector diagram for one phase of PMSM

IV. FAULT MODELING

A. Eccentricity

Eccentricity in a machine is a condition of uneven air-gap between the stator and rotor. If the condition is severe, the Unbalanced Magnetic Pull (UMP) could cause stator and rotor contact [15]. Generally, eccentricity is classified into three types: Static eccentricity, dynamic eccentricity and mixed eccentricity.

Static eccentricity is the case that there is a displacement of the axis of rotation, which usually could be caused by an oval stator or misaligned mounting of bearings, rotors or stators. In this case, the air gap is length is fixed in space. Static eccentricity ratio is defined as [16]

$$\vec{e}_s = \frac{\vec{\varepsilon}_s}{g} \tag{3}$$

where ε_s is the radial distance between rotor axis and stator axis, and g is the uniform air-gap length. So the eccentricity ratio has the limit as follows:

$$0 \le |\vec{e}_s| \le 1 \tag{4}$$

Dynamic eccentricity is the condition in which the stator axis and the rotor rotation axis are identical, but the rotor's axis is displaced to some extent. Therefore the minimum air-gap length position rotates around. This case is usually caused by bent shaft, misaligned mounting of bearings, etc. Similarly, the dynamic eccentricity ratio is defined as

$$\vec{e}_d = \frac{\vec{\varepsilon}_d}{g} = \frac{|\vec{\varepsilon}_d|\angle\omega t}{g} \tag{5}$$

where ε_d is the radical distance between rotor's axis and stator's axis.

Mixed eccentricity is the combination of static and dynamic eccentricity defined by equation 6 and 7 [16].

$$|\vec{e}_m| = \left|\frac{\vec{\varepsilon}_s}{g} + \frac{\vec{\varepsilon}_d}{g}\right| = \sqrt{|\vec{e}_s|^2 + |\vec{e}_d|^2 + 2|\vec{e}_s||\vec{e}_d|\cos(\omega t)} \tag{6}$$

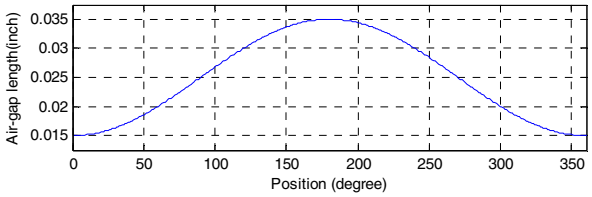

Fig 3. Static air-gap length around the air-gap

$$\angle\varphi = \angle\vec{e}_m = \tan^{-1}\frac{|\vec{e}_d|\sin(\omega t)}{|\vec{e}_s| + |\vec{e}_d|\cos(\omega t)} \tag{7}$$

where φ is the angle of the mixed eccentricity, with a reference to static eccentricity direction. It is a time dependent variant with a period same as rotor. Thus, the air-gap length l could be calculated as

$$l_{air}(\zeta, t) = R_s - |\vec{e}_m| g\cos(\zeta - \varphi) - \sqrt{R_r^2 - |\vec{e}_m|^2 g^2 \sin^2(\zeta - \varphi)} \tag{8}$$

where ζ is the position around the air-gap, from 0 to 360 degree. Figure 3 illustrates the air-gap length of PMSM as a function of position operating with 40% static eccentricity. For dynamic eccentricity air-gap length, it has exactly the same curve but it moves towards one direction at the same speed as the rotor. For mixed eccentricity, the air-gap length is simply the numerical summation of these two minus the average air-gap length.

Magnetic flux is MMF divided by reluctance. In a machine's magnetic circuit, reluctance is a function of the air-gap length and back iron equivalent length l_{iron}, as given by equation 9.

$$\Phi(\zeta, t) = \frac{F}{R_{air} + R_{iron}} = \frac{F}{\frac{l_{air}(\zeta, t)}{\mu_o A_{air}} + \frac{l_{iron}}{\mu_o \mu_r A_{iron}}} \tag{9}$$

where Φ is magnetic flux through a search coil, F is MMF produced by permanent magnets, R_{air} and R_{iron} are reluctance of air-gap and back iron respectively, and μ_o is the permeability of the air, μ_r is the relative permeability of the back iron. If only static eccentricity exists, l_{air} is just a function of position, so Φ is also time irrelevant. If dynamic eccentricity exists, Φ will be a function of both position and time.

B. Armature Winding Short-circuit

Armature winding faults are usually cased by insulation failure. They are commonly classified into phase-to-phase short circuit, phase-to-ground short circuit or inter-turn short circuit [8]. In phase-to-phase short circuit, fuses might burn and machine could stop. In a phase-to-ground short circuit, if machine still runs, large torque ripple can be found. In an inter-turn short circuit, the faulty winding has a smaller number of effective turns than the other healthy windings, so one can find an asymmetry in machine's armature current or armature MMF. This signature is proposed to be used as an indicator in this paper. Figure 4 shows the path for the coupling of flux when only the armature MMFs are considered.

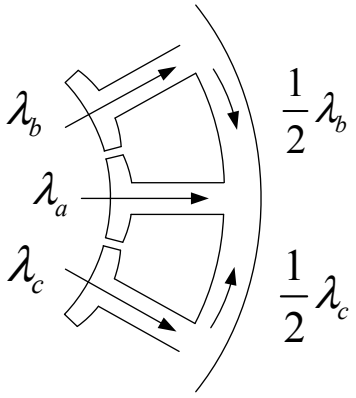

Fig 4. Flux in teeth and back iron

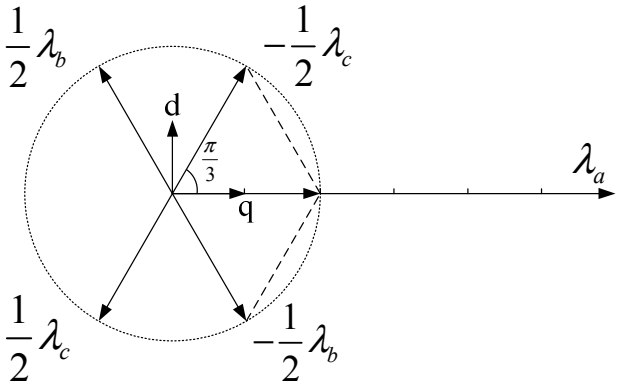

Fig 5. Three phase flux linkage vector summation

Applying KCL, one gets

$$\lambda_A = \lambda_a - \frac{1}{2}\lambda_b - \frac{1}{2}\lambda_c \tag{10}$$

where λ_A is the flux linkage through Teeth A; λ_a is the flux linkage produced by coil around Teeth A; λ_b is the flux linkage produced by coil around Teeth B and λ_c is the flux linkage produced by coil around Teeth C. The phasor diagram for this arrangement is shown in Fig 5. It illustrates that when a phase-to-ground short circuit occurs at phase a, there will still be 1/3 flux linkage produced by adjacent armature winding left. In most cases with low voltage machines, the faults are bolted. If phase b is shorted, there will be 5/6 flux linkages left at q-axis, whereas some d-axis armature MMF component exists.

So the remaining flux linkage λ_f during inter-turn short-circuit can be expressed as

$$\lambda_f = \frac{2N}{3n}\lambda \tag{11}$$

where λ is the flux linkage through the same coil in a healthy machine, N is the total number of turns, and n is the number of shorted turns.

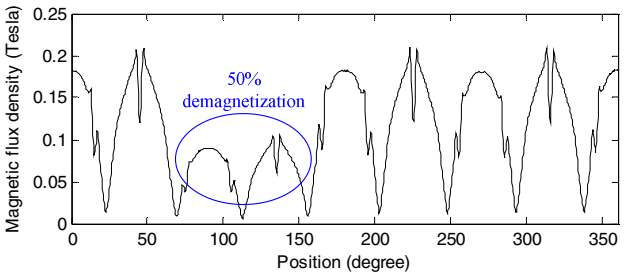

Fig 6. Magnetic flux density around the air-gap

C. *Demagnetization*

The permanent magnets in a PMSM could be demagnetized in applications that require operation at high temperatures, high impropriate armature current, or even by the aging of the magnets themselves [17]. The demagnetization could be uniform over all poles, or partial, over certain region or poles. In this paper, both cases are simulated. For partial demagnetization, two out of eight magnetic poles' coercivity is reduced by 50%. This modifies the magnetic flux density distribution as shown in Fig 6. The small notches in this figure are caused by slot effect. For uniform demagnetization, all the poles' coercivity is reduced by 50%, so the flux density distribution's shape remains the same, except the scale.

V. SIMULATION RESULTS

The search coil mounted PMSM with different fault conditions are simulated using FEA software package MagNet® by Infolytica. The following paragraphs present the measured results from the 2D transient simulation.

Voltage measured across the twelve search coils for different load conditions are illustrated in Fig 7. In each condition, every star represents a search coil. In this polar figure, the amplitude of coil measured voltage is represented by the distance between the star and the figure center, in Volts. It should be noted that the phase of the coil measured in volts is four times the phase of the corresponding star. This is because the phase difference between neighboring stars in this polar figure is 30 degree, whereas the phase difference between neighboring search coils is 120 degree.

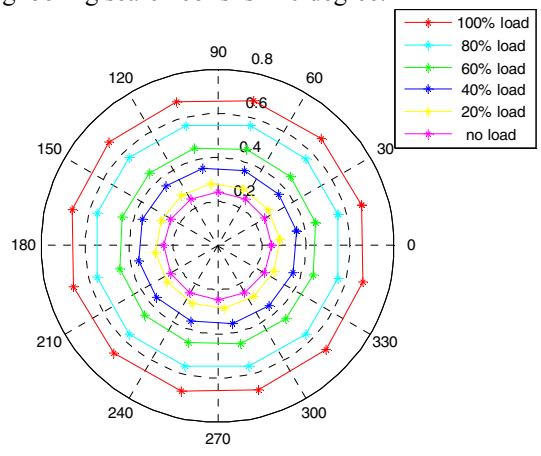

Fig 7. Measured voltage and phase with different load

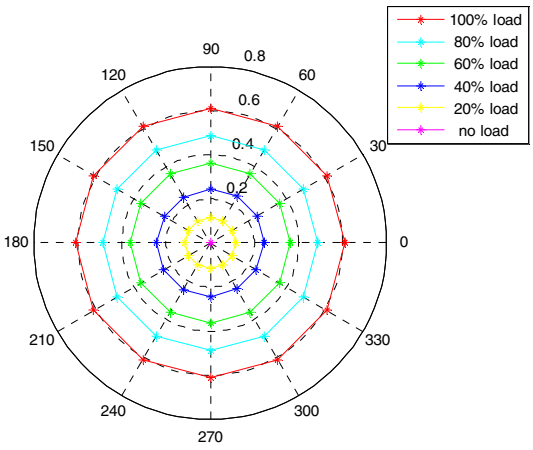

(a)

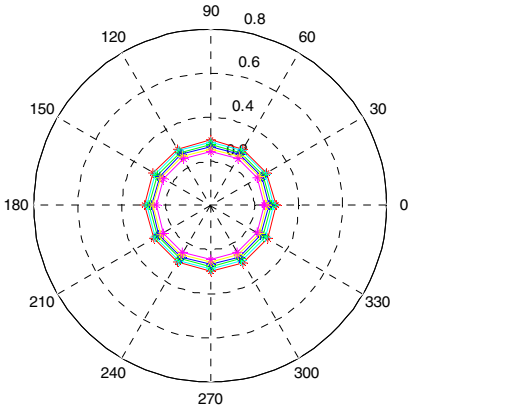

(b)

Fig 8. Decoupled voltage (a) armature component (b) field component

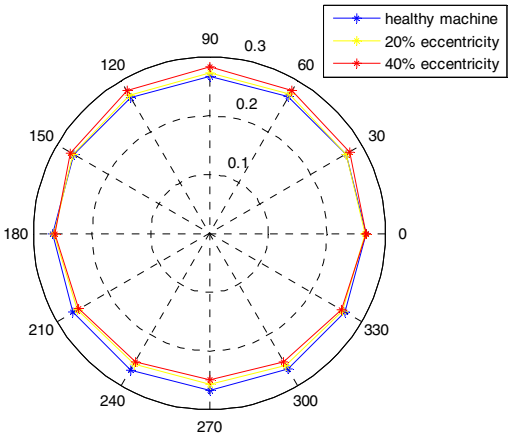

Fig. 9. Field component in a static eccentricity running machine

After decoupling is applied, Fig 7 can be transformed to Fig 8, which is composed by (a) the armature reaction voltage and (b) the field induced voltage. It must be noted that their phases are all zero due to decoupling. These two figures demonstrate that under different load conditions, the armature MMF is proportional to the load while the field MMF remains the same except some disturbance by d axis armature induced MMF.

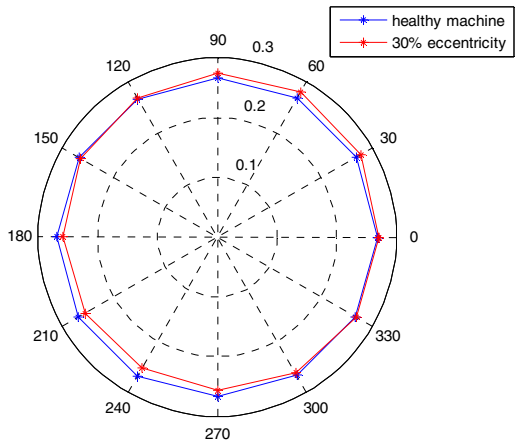

Fig. 10. Field component in a dynamic eccentricity running machine

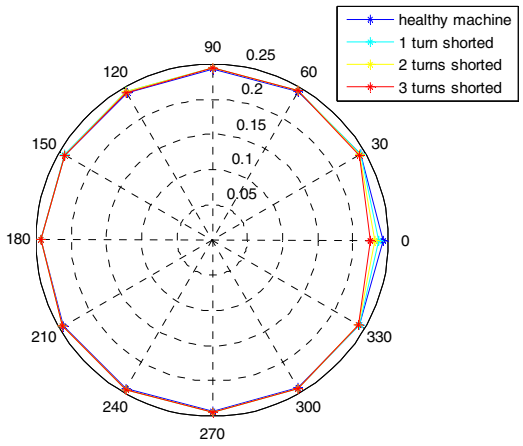

Fig. 11. Armature component in an inter-turn shorted machine

Figure 9 shows the field component of measured voltage of the machine with 0.005 (20%) inch and 0.01 (40%) inch static eccentricity, compared with a healthy one. The eccentricity is in the upward direction, which corresponds to 90 degrees in these phasor diagrams. This slight shift to 90 degree position in this figure can be easily observed.

Figure 10 illustrates the case with a 30% dynamic eccentricity. It can be seen that there is a shift to 45 degree position, which is the direction the rotor shifts towards when the data is collected. In the case of dynamic eccentricity, the shift direction rotates at the synchronous speed. Fig. 10 shows the curve at an arbitrary instant of time.

Figure 11 shows three cases with one, two, and three turns of the armature coils around a tooth, which is at 0 degree position, are inter-turn shorted. A change of Ampere-Turns at that position causes a distortion of armature MMF. It can be seen that the difference of various number of shorted turns can be distinguished, even only one out of thirty turns is shorted.

Figure 12 shows a case where one of the three phases is grounded. As explained in Section IV, 1/3 of the magnitude of the flux linkage is remaining at the teeth of phase A, at the position 0, 90, 180 and 270 degree, produced by the neighboring phases, whereas 5/6 of the flux linkage is remaining at the teeth of phase B and phase C.

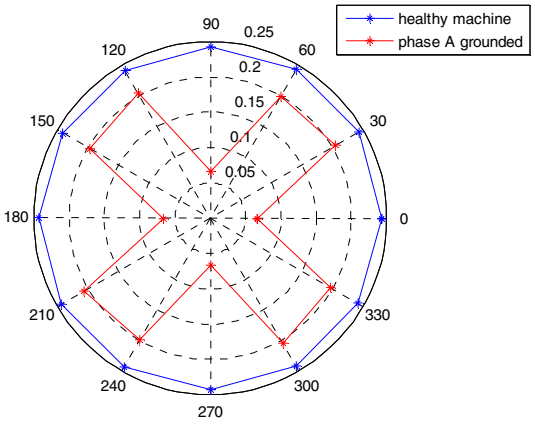

Fig 12. Armature component in a one phase grounded machine

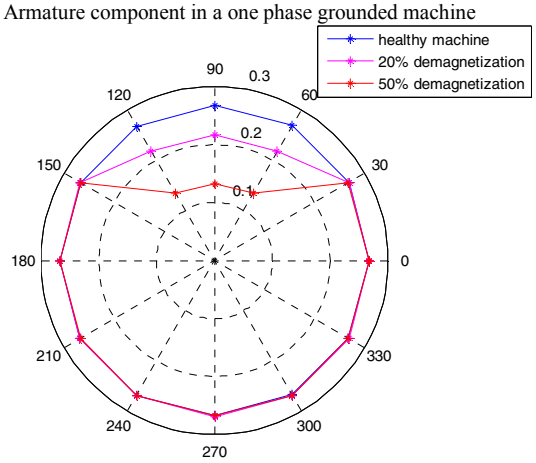

Fig 13. Field component in a one pole pair demagnetized machine

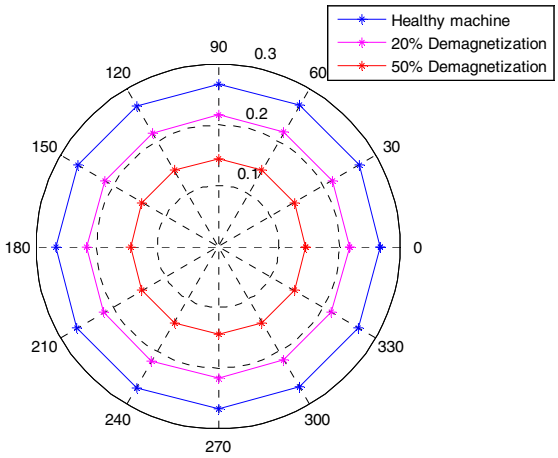

Fig. 14. Field component in a uniform demagnetized machine

Figure 13 presents the field component of the measured voltages in a partial demagnetized machine, in which one out of the four pole pairs is 20% and 50% demagnetized respectively. Since the rotor is revolving at the synchronous speed, the curves in this figure are time variant, revolving at the synchronous speed while retaining its shape. Figure 13 just showed the curve at an arbitrary time instant.

Figure 14 presents the field component of measured voltages in a uniformly demagnetized machine, in which all

the poles are 20% and 50% demagnetized respectively. Since the poles are in uniform demagnetization, even though the red curve in this figure revolves at the synchronous speed, it exhibits the same shape. Therefore, deterioration in magnetic performance of the permanent magnets can be detected from the field component of coils measured voltages.

VI. CONCLUSIONS

In this paper, a novel scheme for PMSM health monitoring and fault diagnosis is proposed. Search coils are designed to be mounted around each tooth so that the air-gap flux density can be measured. Only first order harmonic is used for fault detection so that it is immune to the harmonics induced by power electronic devices. Another benefit of this technique is that the load condition does not necessarily need to be specified for accurate fault diagnosis.

2D time transient FEA simulations have been presented for the verification of proposed method over different motor operation conditions. The faults considered in this study include static and dynamic eccentricity, inter-turn short circuit, phase-to-ground short circuit, partial and uniform demagnetization. Results show that the signatures of different faults are easy to identify, so no time-consuming pattern recognition algorithm is required. Furthermore, the direction of eccentricity and the location of winding shorted turns can be found. In addition, this method is also capable of evaluating the severity of each fault, which is of significant importance in mission critical applications such as automotive, aerospace and military applications. The drawback of this method is that it is invasive, so it might not be very economical for the machines that have already been manufactured, but holds potential for emerging applications.

APPENDIX

The specifications of the presented PMSM are summarized in Table II.

TABLE II

SPECIFICATIONS OF THE PRESENTED PMSM

Number of poles pairs	4
Phases	3
Number of stator slots	12
Rated power	675W
Rated current	15A
Rated speed	2800rpm
Rated torque	2.3Nm
Rated frequency	60Hz

REFERENCES

[1] R. R. Schoen, B. K. Lin, T. G. Habetler, J. H. Schlag and S. Farag "Motor bearing damage detection using stator current monitoring" *IEEE Trans. Ind. Applica.*, vol. 31, no. 6, pp. 1274–1279, Nov.-Dec. 1995.

[2] G. M. Joksimovic, and J. Penman, "The Detection of Inter-Turn Short Circuits in the Stator Windings of Operating Motors" *IEEE Trans. Indus. Electron.*, vol. 47, no. 5, pp. 1078–1084, Oct. 2000

[3] W. L. Roux, R. G. Harley, and T. G. Habetler, "Detection rotor faults in low power permanent magnet synchronous machines," *IEEE Trans. Power Electron.*, vol. 22, no. 1, pp. 322–328, Jan. 2007.

[4] R. A. Leonhard and W. T. Thompson, "Vibration and stray flux monitoring for unbalanced supply and inter-turn winding fault diagnosis in induction machines," *British J. Non-Destructive Testing*, pp. 211–215, Jul. 1986.

[5] D. Filbert, "Intelligent measurement methods in technical diagnosis and quality assurance—A comparison," *Measurement*, vol. 6, no. 2, pp. 69–74, Apr.-Jun.1988.

[6] J. Penman, M. N. Dey, A. J. Tait, and W. E. Bryan, "Condition Monitoring of Electrical Drives", *Proc. IEE*, vol. 133, pt. B, pp. 142-148, May 1986.

[7] J. Penman, H. G. Sedding, B. A. Lloyd, and W. T. Fink, "Detection and location of interturn short circuits in the stator windings of operating motors," *IEEE Trans. Energy Conv.*, vol. 9, pp. 652–658, Dec. 1994.

[8] G. B. Kliman, W. J. Premerlani, R. A. Koegl, and D. Hoeweler, "A new approach to on-line turn fault detection in ac motors," in *Proc. Conf. IEEE-IAS Annu. Meeting*, vol. 1, pp. 687–693, Oct. 1996.

[9] J. L. Kohler, J. Sottile, and F. C. Trutt, "Alternatives for assessing the electrical integrity of induction motors," *IEEE Trans. Ind. Applica.*, vol. 28, pp. 1109–1117, Sept.-Oct. 1992.

[10] J. Sottile and J. L. Kohler, "An on-line method to detect incipient failure of turn insulation in random-wound motors," *IEEE Trans. Energy Conv.*, vol. 8, pp. 762–768, Dec. 1993.

[11] M. A. Cash, T. G. Habetler, and G. B. Kliman, "Insulation failure prediction in AC machines using line-neutral voltages," *IEEE Trans. Ind. Applica.*, vol. 34, pp. 1234–1239, Nov.-Dec. 1998.

[12] D. Filbert, "Advanced fault diagnosis for the mass production of small power electric motors," in *Proc. Electro Motion*, vol.2, no.3, pp. 159–166, 1995

[13] C. Schneider and D. Filbert, "Parameter estimation and residual analysis a comparison," in *Proc. IFAC Fault Detection, Supervision and Safety for Technical Processes*, pp. 701–705, Jun. 1994.

[14] H. Saadat, *Power System Analysis.* McGraw Hill, 2002.

[15] T. G. H. C. Kral, and R. G. Harley, "Detection of Mechanical Imbalances of Induction Machines Without Spectral Analysis of Time-Domain Signals," *IEEE trans. Ind. Applica.*, vol. 40, Jul.-Aug. 2004.

[16] B. M. Ebrahimi, J. Faiz, and M. J. Roshtkhari, "Static-, dynamic-, and mixed-eccentricity fault diagnosis in permanent-magnet synchronous motors," *IEEE Trans. Ind. Elec.,* vol. 56, no. 11, Nov. 2009.

[17] J. Farooq, S. Srairi, A. Djerdir, and A. Miraoui, "Use of permeance network method in the demagnetization phenomenon modelling in a permanent magnet," *IEEE Trans. Magn.*, vol. 42, no. 4, pp. 1295–1298, Apr. 2006.